University of Baghdad
College of Engineering
JOURNAL OF ENGINEERING

Journal of Engineering

journal homepage: www.jcoeng.edu.iq

Volume 31 Number 4 April 2025

Realization of Current-Mode Inverting and Non-inverting Schmitt Trigger Circuit using Current Follower Transconductance Amplifier (CFTA)

Amira R. Hamad

Department of Electrical Engineering, College of Engineering, Salahaddin University, Erbil, Iraq

ABSTRACT

This article proposes a current mode inverting and non-inverting Schmitt trigger circuit, which utilizes a Current Follower Transconductance Amplifier (CFTA) and its application in square and triangular wave generators. The hysteresis of a Schmitt trigger is directly influenced by the process variations and transistor mismatches. This issue is more challenging in applications where the level of noise and disturbances is not predictable. To overcome this deficiency, Schmitt triggers with tunable hysteresis can be used as a practical solution. The suggested circuit consists of a single CFTA analog building block laterally with one grounded resistor. The grounded resistor makes the realization of the above-mentioned circuit possible. The proposed circuit has low input impedance and high output impedance, which is preferred in current mode (CM) circuits. It is characterized by adjustable thresholds and low power consumption. It provides both inverting and non-inverting responses without extra floating elements. Additionally, it has electronically adjustable threshold levels and a wide bandwidth. All these specifications have been validated through PSPICE simulations. The design focuses on reducing power consumption by incorporating active elements and grounded resistors. It's Optimizing for low voltage operation, while effectively managing current to ensure high performance without excessive energy use. It is an efficient and low-power method for generating square and triangular waves. The PSPICE simulation results are illustrated, and the given results coincide well with the theoretical expectation. The total power consumption is 1.26mW at ±1.5V supply voltage.

Keywords: Schmitt trigger, CFTA, Current mode.

1. INTRODUCTION

This article proposes using current-mode active components, specifically the current follower transconductance amplifier (CFTA), in analog electronic circuits to achieve a larger dynamic range and high bandwidth. The CFTA is highlighted as being particularly beneficial

*Corresponding author
Peer review under the responsibility of University of Baghdad.
https://doi.org/10.31026/j.eng.2025.04.06

Article received: 21/08/2024
Article revised: 15/12/2024
Article accepted: 15/02/2025
Article published: 01/04/2025

in applications such as oscillators and filters **(Daibor et al., 2008; Sotner et al., 2009; Silapan et al., 2011; Singh et al., 2013; Nisha et al., 2015; Singh et al., 2016; Kumari et al., 2017; Özer, 2021; Prasad et al., 2021; Tasneem et al., 2022; Başak et al., 2022; Demirel et al., 2023)**. The regenerative comparator, also known as the Schmitt trigger, was advanced by Otto Schmitt in the 1930s. This component is commonly utilized in communication circuits and signal processing to enhance control and minimize noise. Additionally, it finds applications in frequency doublers, image sensors, and wireless transponders **(Chavez, 1995; Akter et al., 2008; Choi et al., 2009; Yuan, 2009; Janveja et al., 2016; Wassan et al., 2012; De Marcellis et al., 2017)**. For the previous two decades, the demand for low-voltage portable and battery-powered equipment has augmented drastically. Therefore, researchers have been keen on lowering the supply voltage of analog circuits. As a low-voltage operative circuit becomes essential, the current mode (CM) technique is suitable for this resolution **(Biolek, 2003)**. To conquer the operational amplifier building block handicaps and to get high-speed systems, the analog electronic circuit engineers observed for additional capabilities and extra building blocks **(Biolek, 2003; Keskin et al., 2006; Tangsrirat et al., 2007; Bang et al., 2014; Thakur et al., 2021; Fathima et al., 2022; Lin et al., 2023; Mohammed et al., 2024)**. Many papers related to Schmitt Trigger using voltage differencing transconductance amplifier VDTA, current differencing transconductance amplifier CDTA, and Z copy current differencing buffer amplifier (ZCCDBA) are available in the literature. The CM Inverting and non-inverting Schmitt trigger configuration utilizing a CFTA as active elements is a novel approach in circuit design. This circuit offers unique advantages over traditional configurations by utilizing only active elements and grounded resistors, eliminating the need for additional sub-circuit elements. The ability to provide both inverting and non-inverting responses, coupled with low voltage and power consumption, wide bandwidth, and electronically adjustable threshold levels, makes this design stand out in the field of Schmitt trigger circuits.

Schmitt triggers are susceptible to hysteresis issues caused by process variations and transistor mismatches, particularly in environments with unpredictable noise (**Yuan, 2010a**). Implementing tunable hysteresis in Schmitt triggers can mitigate these challenges (**Amiri et al., 2020**), leading to improved performance and reduced power consumption in various applications, including power amplifier circuits **(Yuan, 2010b; Radfar et al., 2020)**. In this paper, detailed analysis and simulation results of the proposed circuit are presented. The theoretical analysis is compared with PSPICE simulation results, to validate the functionality and performance of the CM Inverting and non-inverting Schmitt trigger configurations. Additionally, we discuss the implications and potential applications of this circuit design in various electronic systems. Through this study, we demonstrate that the CM Inverting and non-inverting Schmitt trigger circuit based on a CFTA offers a simple, efficient, and high-performance solution compared to existing Schmitt trigger circuits. The proposed circuit contains one CFTA active building block with only one grounded passive component.

2. COMPARISONS WITH AVAILABLE SCHMITT TRIGGER CIRCUIT

The proposed CM Inverting and non-inverting Schmitt trigger circuit utilizing a CFTA offers advantages over existing Schmitt trigger circuits. A key comparison is the use of only one grounded passive component in the proposed circuit, while other circuits utilize floating passive components. Additionally, existing circuits often require multiple passive components like resistors, which increase complexity, unlike the given circuit. Furthermore,

the proposed circuit operates in CM, distinguishing it from voltage-mode (VM) circuits, and provides both inverting and non-inverting responses simultaneously, a feature that is not found in many existing Schmitt trigger circuits.

- The Schmitt trigger circuits **(Pal et al., 2015; Madeira et al., 2016; Nagalakshmi et al., 2018; Ranjan et al., 2018; Srinivasulu et al., 2020)** require more than one passive component like a resistor which increases the overall complexity of the circuit.
- The Schmitt trigger circuit reported by **(Pal et al., 2015; Siripruchyanun et al., 2015; Kumar et al., 2017; Ranjan et al., 2018; Nagalakshmi et al., 2018; Maheswari et al., 2019; Srinivasulu et al., 2020; Kannaujiya et al., 2024)** is operating in VM, whereas the proposed circuit Operating in CM.
- The Schmitt trigger circuit reported by **(Siripruchyanun et al., 2015; Madeira et al., 2016; Das et al., 2017; Kumar et al., 2017; Nagalakshmi et al., 2018; Maheswari et al., 2019**) Provides only inverting or non-inverting Schmitt trigger whereas the proposed circuit Providing inverting and non-inverting Schmitt trigger responses Simultaneously.
- The Schmitt trigger circuit reported by **(Pal et al., 2015; Madeira et al., 2016; Ranjan et al., 2018; Nagalakshmi et al., 2018; Srinivasulu et al., 2020)** utilizes of floating passive component whereas the proposed circuit uses only one grounded passive component. A summary of the comparative study is given in **Table 1**.

Table 1. Comparative study of the available Schmitt trigger circuit

References	Active Components Required	Passive Elements Required	ALL-Grounded Passive Compt.	Power Supply	Employing the CM	Inverting/non-inverting Schmitt trigger responses
(Pal et al., 2015)	1 CDBA	3-R	NIL	±10 V	NIL	Both
(Siripruchyanun et al., 2015)	1-VDTA	1-R	YES	±1.5V	NIL	INV
(Madira et al., 2016)	ZC-CDTA	2-R	NIL	± 0.85	YES	INV
(Kumar et al., 2017)	MO-CFDITA	1-R	YES	±10 V	NIL	Both
(Kumar et al., 2017)	DXCCTA	NIL	-	±1.25 V	YES	Non-INV
(Das et al., 2017)	CCCDTA	NIL	-	±1 V	YES	INV.
(Ranjan et al., 2018)	1-FTFN	2-R	-	± 1.65	NIL	Both
(Nagalakshmi et al., 2018)	1-CDTA	2-R	NIL	±2.5 V	NIL	INV.
(Maheswari et al., 2019)	ZC-CDBA	NIL	-	±0.8 V	NIL	INV.
(Srinivasulu et al., 2020)	1-CCCII	2R	NIL	± 2 V	NIL	Both
(Kannaujiya et al., 2024)	CMOS	-	-	1V	NIL	Both
(Proposed circuit)	1-CFTA	1-R	YES	±1.5 V	YES	Both

3. METHODOLOGY

3.1 Current Follower Transconductance Amplifiers (CFTA)

The CFTA **(Daibor et al., 2008; Nisha et al., 2015)** is a four-pin network with ideal characteristics represented by a specific matrix; it is a useful building block in analog circuit design. **Fig. 1** displays the electrical symbol and equivalent circuit of this network.

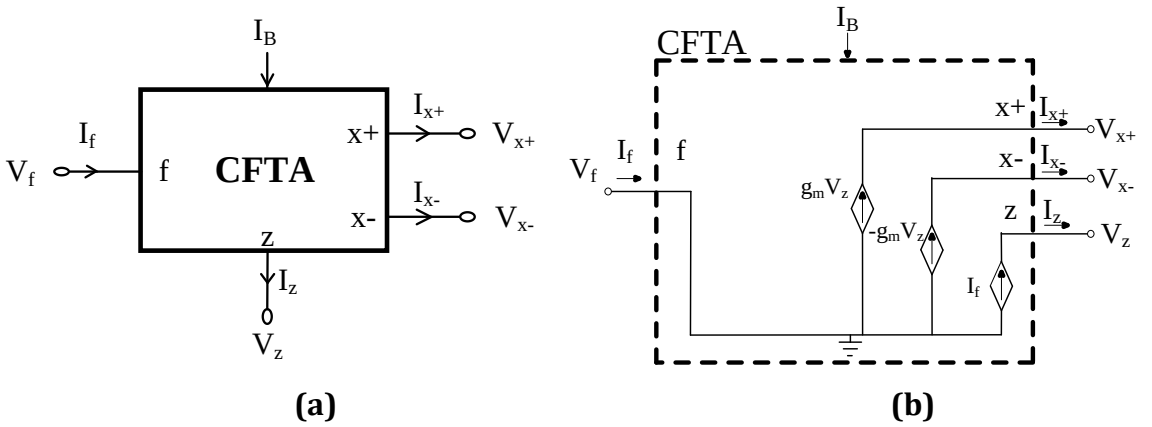

Figure 1. CFTA (a) Symbol (b) Equivalent Circuit

The CFTA's input stage acts as a current follower with low input impedance, this allows higher transient currents to flow into the amplifier as needed, transferring current to a high-impedance intermediate Z-terminal. The transconductance stage (g_m), controlled by a bias current (I_B), transforms the voltage drop across the grounded impedance into output currents Ix+ and Ix-.
The following matrix characterizes the terminal relations for

$$\begin{bmatrix} V_f \\ I_z \\ I_{x+} \\ I_{x-} \end{bmatrix} = \begin{bmatrix} 0 & 0 & 0 & 0 \\ 1 & 0 & 0 & 0 \\ 0 & +g_m & 0 & 0 \\ 0 & -g_m & 0 & 0 \end{bmatrix} \cdot \begin{bmatrix} I_f \\ V_Z \\ V_{x+} \\ V_{x-} \end{bmatrix}$$

Where

- g_m is the transconductance gain of the CFTA, which is given by Eq. (1)

$$g_m = \frac{I_B}{2V_T} \tag{1}$$

- V_T: the thermal voltage ($V_T = 26mV$ at room temperature)
- I_B: the external bias current directly influences the transconductance gain g_m of the CFTA

3.2 Proposed Schmitt Trigger Circuit and Its Operation

The proposed circuit contains of a one CFTA active building block with only one grounded passive component as shown in **Fig. 2**. The circuit operates in CM, with the non-inverting terminal treated as port F. A sinusoidal input is applied to the F terminal, which has low impedance. The outputs are taken from the X+ terminal and the X- terminal providing dual output current responses simultaneously. The saturation levels of output currents are determined by the exterior bias current I_B changing the transconductance of the CFTA. The Schmitt trigger electronics circuit which is proposed in the article is shown in **Fig. 2**. The proposed circuit operation is explained thus. The dual saturation levels of output currents I_{out+} and I_{out-} are I_{Sat+} and I_{Sat-}. The dual saturation levels for output currents are given as $I_{sat+} = +I_B$ and $I_{sat-} = -I_B$ for I_{out+} and I_{out-} , respectively.

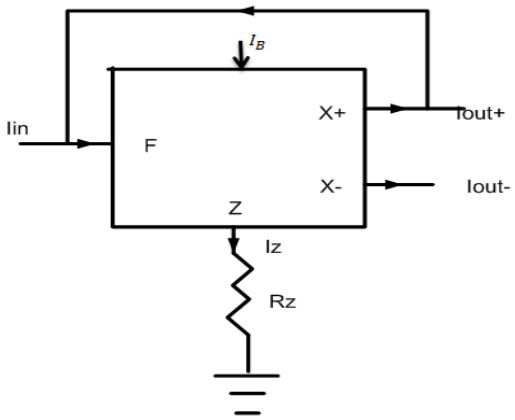

Figure 2. Proposed CFTA Schmitt triggers circuit.

The transfer function of the **Fig. 2** is given in Eq. (2).

$$\frac{I_{out}}{I_{in}} = \frac{g_m R_z}{1-g_m R_z} \tag{2}$$

Hence the Upper Triggering Point (UTP) and Lower Triggering Point (LTP) equations for the proposed circuit of **Fig. 2** are given in Eq. (3) and Eq. (4)

$$UTP = \frac{g_m R_z}{1-g_m R_z} * (+I_B) \tag{3}$$

$$LTP = \frac{g_m R_z}{1-g_m R_z} * (-I_B) \tag{4}$$

The amplitude of the non-inverting Schmitt trigger (I_{out+}) is given in Eq. (5)

$$I_{out+} = \begin{cases} I_{sat+} = I_{B+} \; for \; I_{in} \geq I_{UTP} \\ I_{sat-} = I_{B-} \; for \; I_{in} \leq I_{LTP} \end{cases} \tag{5}$$

The amplitude of inverting Schmitt trigger (I_{out-}) is given in Eq. (6)

$$I_{out-} = \begin{cases} I_{sat+} = I_{B+} \; for \; I_{in} \leq I_{LTP} \\ I_{sat-} = I_{B-} \; for \; I_{in} \geq I_{UTP} \end{cases} \tag{6}$$

Where

R_z is grounded resistor connected at z-terminal.
I_{Sat+} and I_{Sat-} are the positive and negative saturation current, respectively.
I_{out+} and I_{out-} are the non-inverting and inverting output current, respectively.
I_{B+} and I_{B-} are the positive and negative peak bias current, respectively.

4. SIMULATION RESULTS AND DISCUSSION

4.1 Proposed Schmitt Trigger

PSPICE software was used to simulate the proposed circuit. The simulation utilized a CMOS structure of **Fig. 3,** and the dimensions of the transistors are given in **Table 2 (Daibor et al., 2008; Nisha et al., 2015)**. The CFTA CMOS transistor model parameters are given by TSMC

0.25µm CMOS process. The circuit was simulated with supply voltages of VDD = -VSS = 1.5V and a bias current of IB = 28µA. Transient curves for both inverting and non-inverting Schmitt trigger responses were obtained, showing the simultaneous operation of both responses. Additionally, the DC transfer characteristics for both inverting and non-inverting Schmitt trigger responses were analyzed, confirming the circuit's functionality and performance. The proposed circuit in **Fig. 2** was simulated in PSICE software, the input current is a sinusoidal waveform with a frequency of 30 kHz and ±50uA amplitude and an external grounded resistor of $R_z = 10k\Omega$ used in the simulation. The transient curves or inverting and non-inverting Schmitt triggers circuit are shown in **Figs. 4 and 5** Additionally, the observed DC transfer characteristic for inverting I_{OUT-} and non-inverting output Schmitt trigger I_{OUT+} are shown in **Figs. 6 and 7**, respectively. The frequency band for the output response is shown in **Fig. 8**, it defines the range of frequency and above that the proposed circuit works successfully. Furthermore, it shows the effect of electronically controllable upper and lowers triggering points and maximum saturation levels. The proposed circuit was simulated in different bias currents of 20uA, 28uA, and 35uA. The result is shown in **Fig. 9** which shows different upper and lower triggering points. It is evident that the electronically controllable solution is quite simple, and the total power dissipation by the proposed circuits is 1.26mW. The low power dissipation is due to CM operation and the non-inverting DC transfer characteristic of the proposed circuit for different I_B is exposed in **Fig. 10**. Additionally, the variations of threshold current levels against bias current are shown in **Fig.11**. The effect of high input frequency on the waveform distortion, current amplitudes, and possible shifting of threshold levels was simulated for the proposed circuit at an input frequency of 1MHz and current of ±50uA. The simulation result is shown in **Fig. 12,** it is obvious that the frequency response of the proposed circuit depended on the frequency responses of the building blocks.

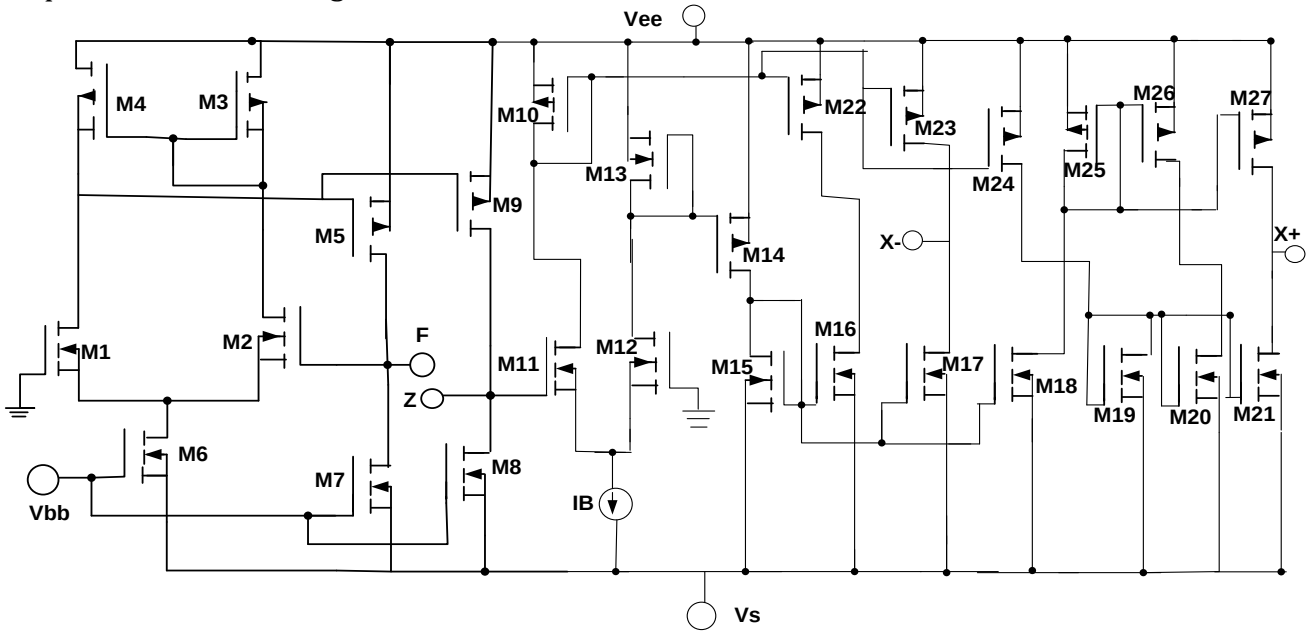

Figure 3. The CMOS structure of CFTA

Table 2. Dimensions of the transistors

Transistor	W (um)	L (um)
M1-M2, M19-M20	1	0.25
M3-M5, M9-M10, M13, M22-M27	5	0.25
M6-M8, M15-M21	3	0.25
M11-M12	25	0.25
M14	4.5	0.25

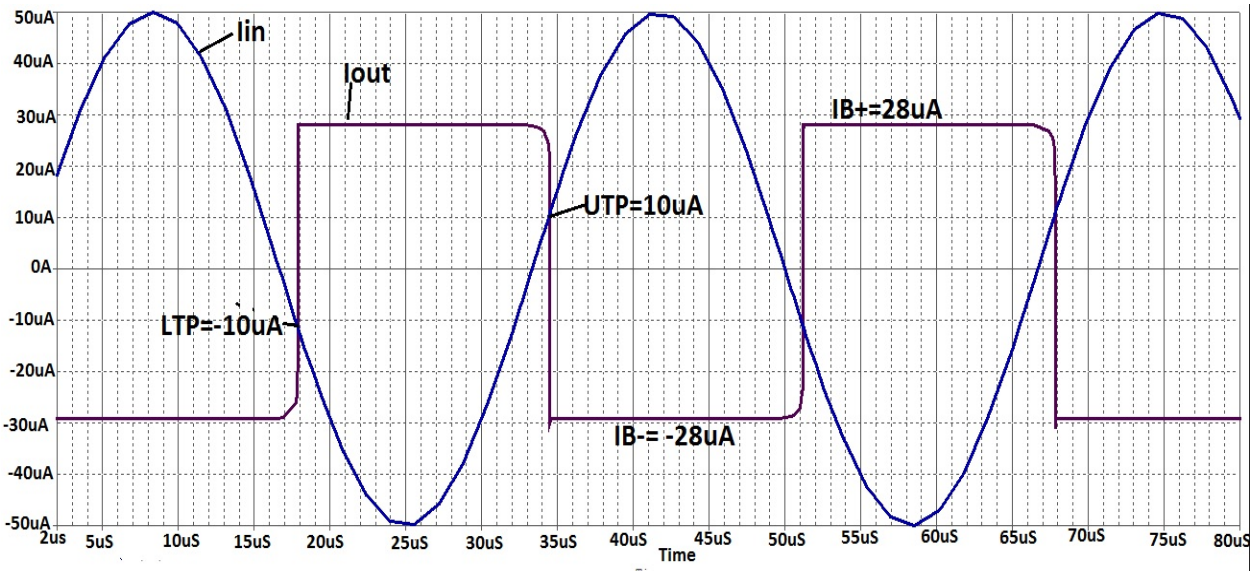

Figure 4. Input (I_{in}) and output (I_{out-}) curves of the inverting Schmitt trigger circuit

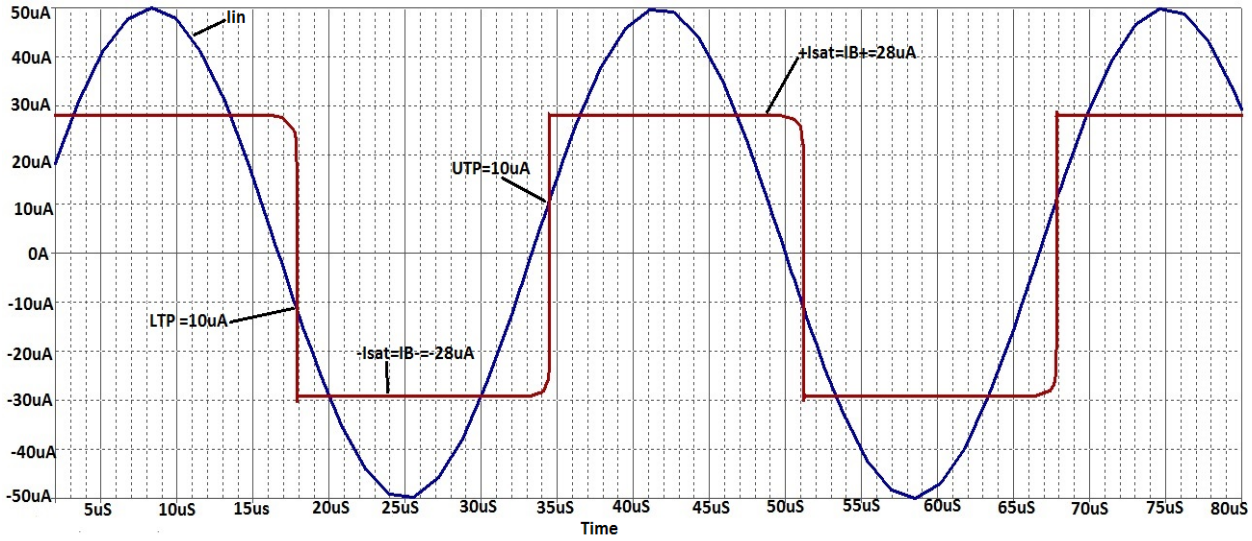

Figure 5. Input (I_{in}) and output (I_{out+}) curves of the non-inverting Schmitt trigger circuit.

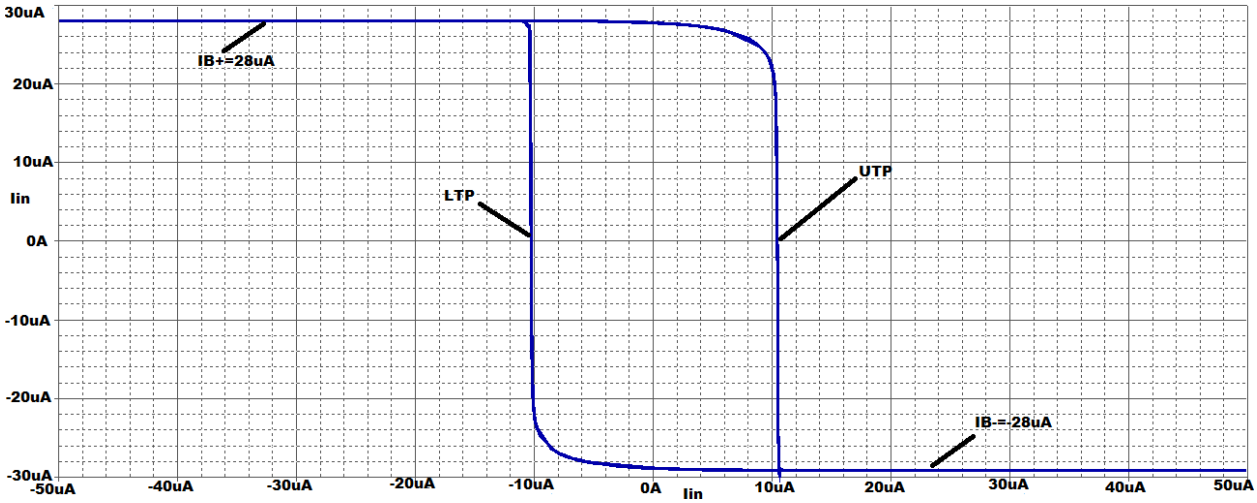

Figure 6. Inverting the DC transfer characteristic of the proposed Schmitt trigger circuit when $I_B = 28uA$

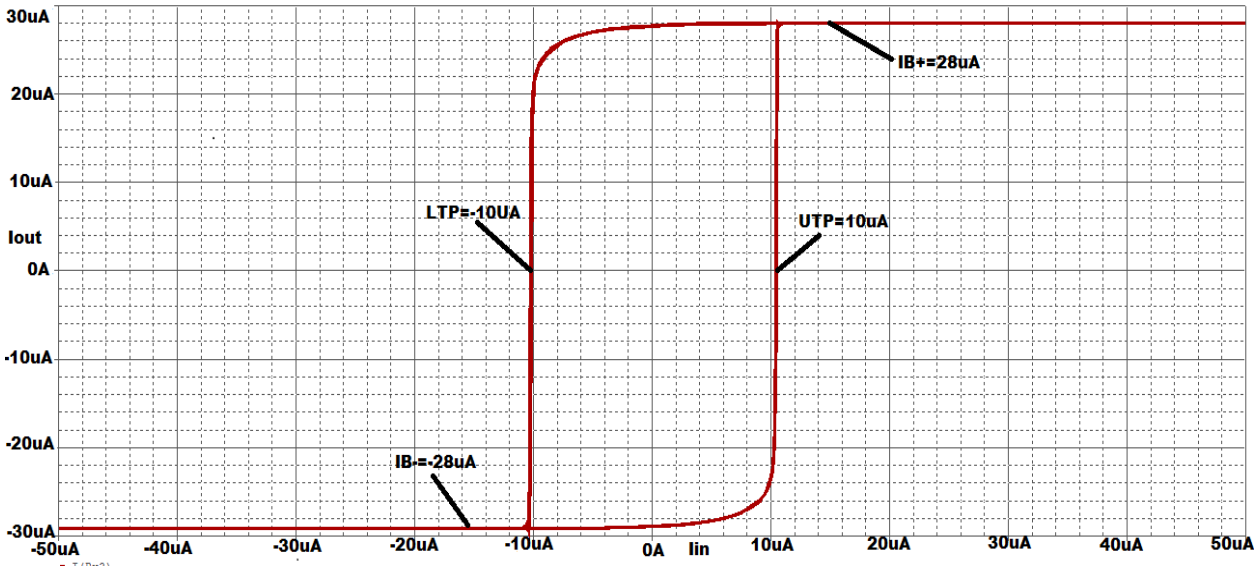

Figure 7. Non-inverting DC transfer characteristic when $I_B = 28uA$

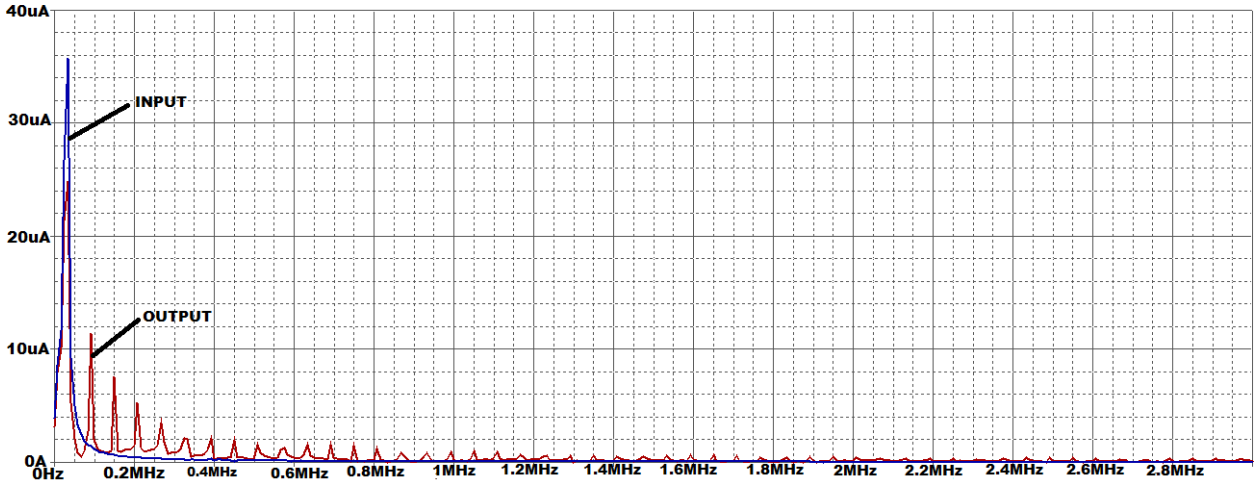

Figure 8. The frequency spectrum of the proposed circuit.

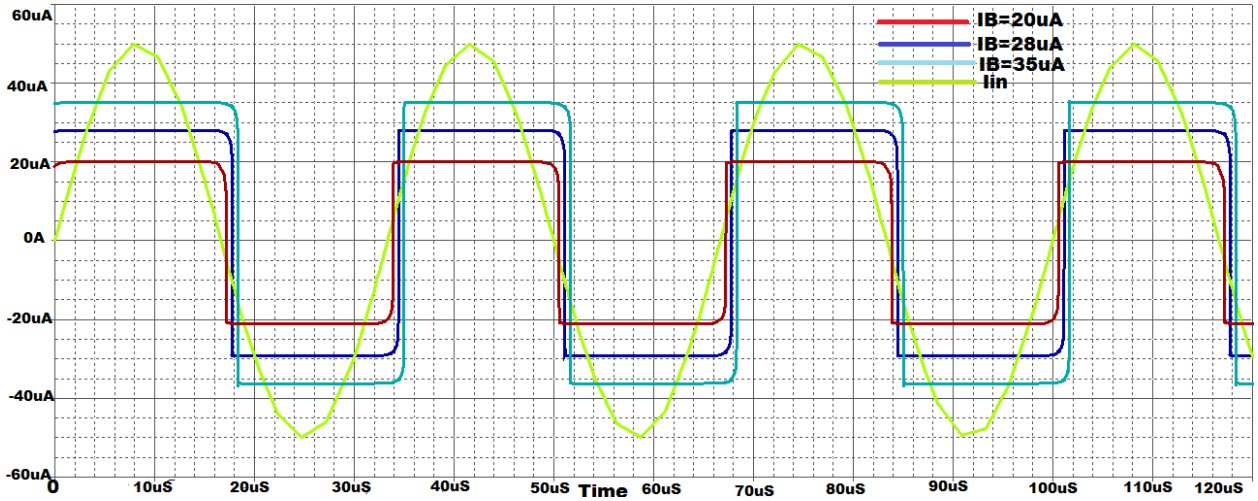

Figure 9. Input(I_{in})and output (I_{out-}) curves of the non-inverting Schmitt trigger proposed circuit for different I_B.

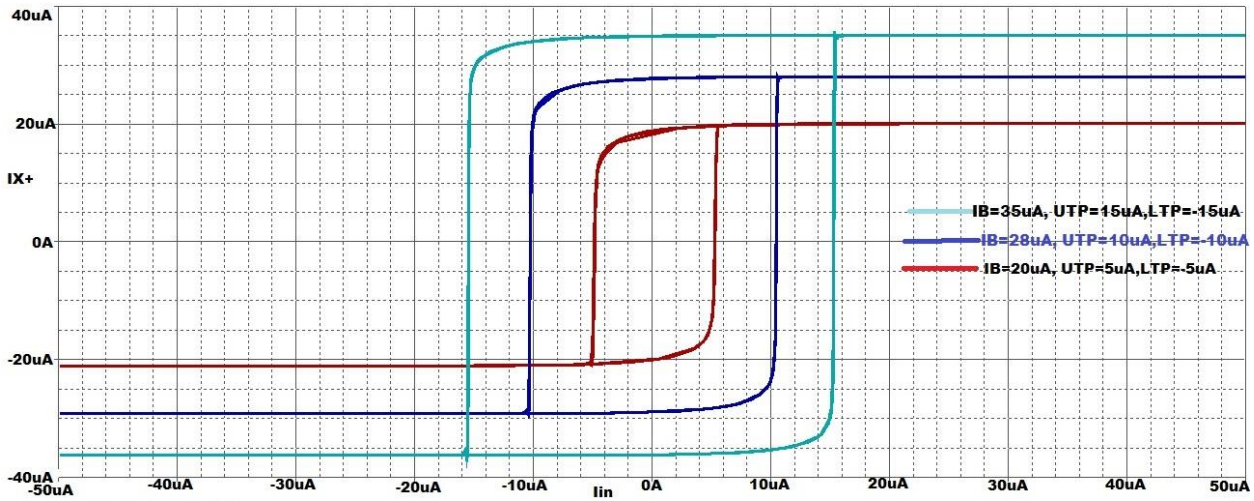

Figure 10. Non-inverting DC transfer characteristic of the proposed Schmitt trigger circuit for different I_B

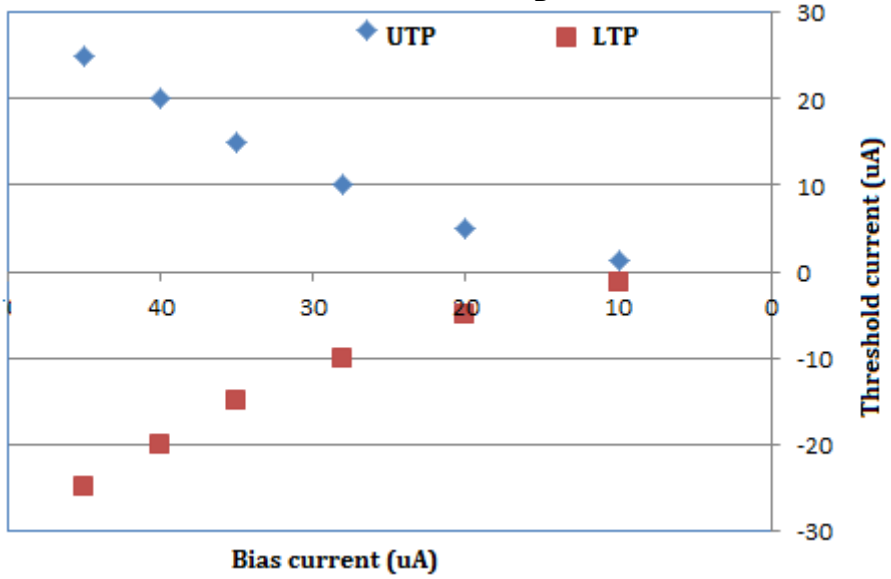

Figure 11. The variations of threshold current levels against bias current

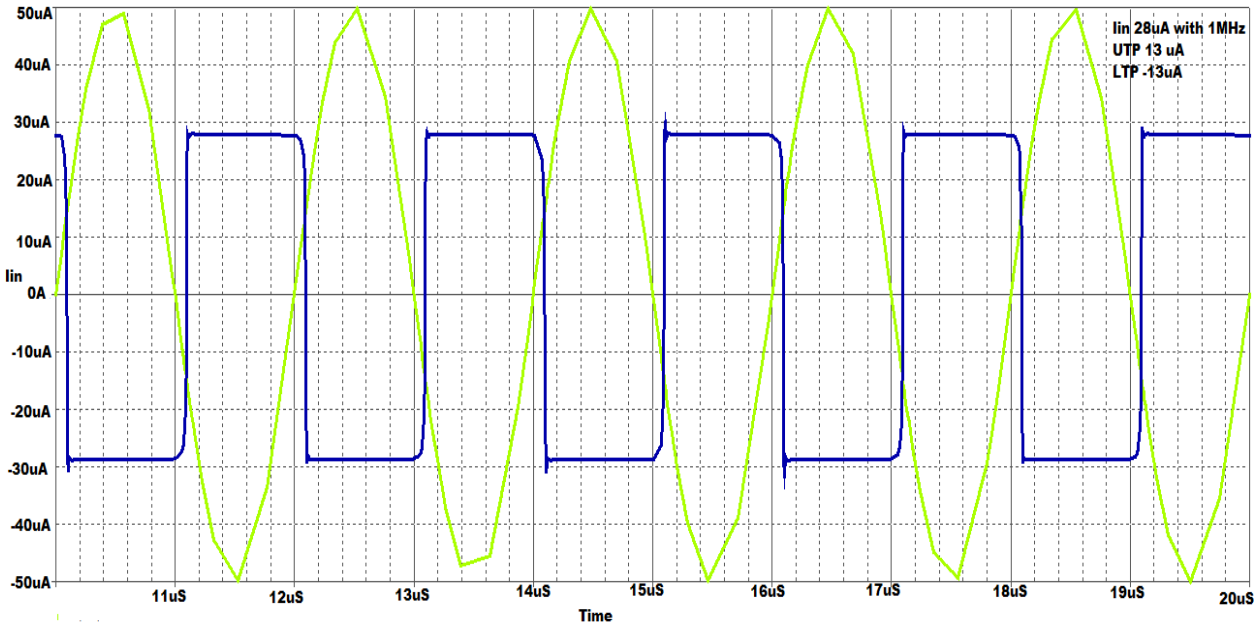

Figure 12. Input current (I_{in}) curve of the proposed inverting Schmitt trigger for input frequency 1MHz

4.2 Application as Waveform Generator

The Schmitt trigger-based CFTA contributes to the generation of square and triangular waves by utilizing feedback mechanisms that create hysteresis in the circuit as shown in **Fig.13**. This hysteresis allows the circuit to switch states at different current levels, which is essential for producing square waves. Additionally, by incorporating a capacitor at the Z terminal of the CFTA2, the circuit integrates the square wave output to generate a triangular wave. The outputs for the square and triangular waves are taken from Iout1 and Iout2, respectively.

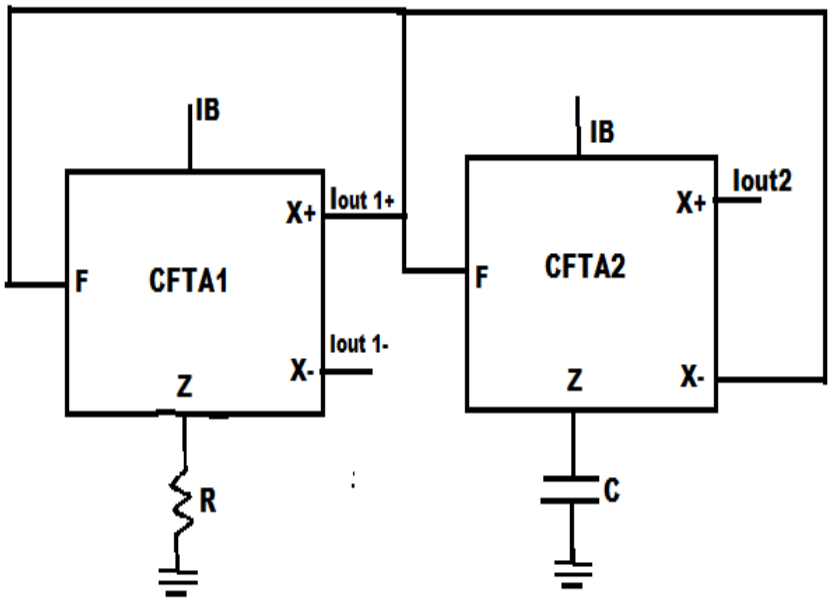

Figure 13. Square and triangular waveform generator

Routine circuits analysis and from the ideal behavior of CFTA given in the above matrix it is easy to derive the transfer function and characteristic equation of **Fig. 13** in the form

$$Transfer\ function = \frac{g_{m1}g_{m2}R}{g_{m1}g_{m2}R+S(C-g_{m1}RC)} \quad (7)$$

where $g_{m1}\ and\ g_{m2}$ are the transconductance of the CFTA1 and CFTA 2, respectively.
R is the grounded resistor connected at the z-terminal of CFTA1
C is the grounded capacitor connected at the z-terminal of CFTA2
From the above transfer function, it is clear that the characteristic equation of **Fig. 13** in the form:

$$g_{m1}g_{m2}R + S(C - g_{m1}RC) = 0 \quad (8)$$

Substituting $s = j\omega$, where ω is the angular frequency in rad/s, from the above Eq. (8), the oscillation frequency (f) is written as:

$$f = \frac{g_{m1}g_{m2}R}{2\pi C\ (g_{m1}R-1)} \quad (9)$$

Fig. 14 shows the simulation result for the waveform generator the element values are designated as R = 10kΩ and C = 100pf. To show the effect of capacitor Value on the oscillation frequency simulates the proposed waveform generator in different capacitors 100pf, 150pF, and 200pF.
The result is shown in **Figs. 15** and **16** which shows different oscillation frequencies. The capacitor value is inversely proportional to frequency oscillation.

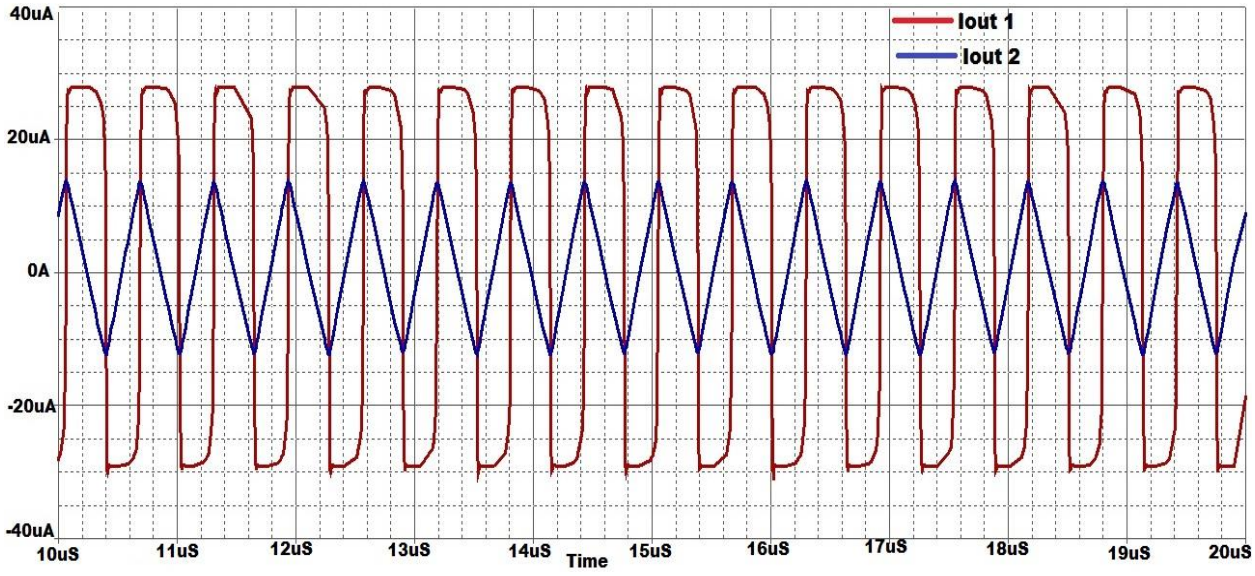

Figure 14. Square and triangle waveform generator

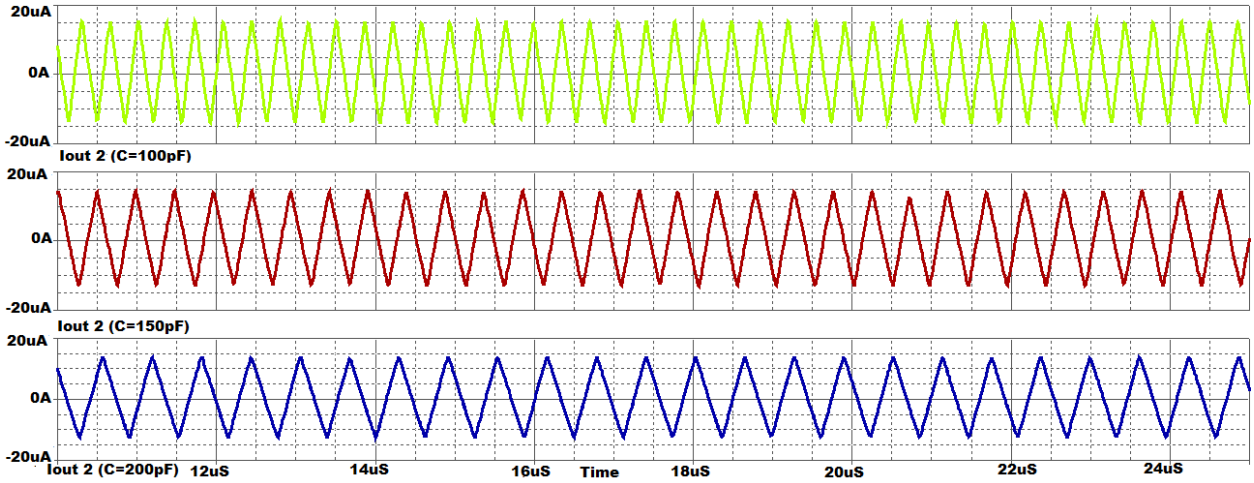

Figure 15. Triangle waveform generator for different capacitor values.

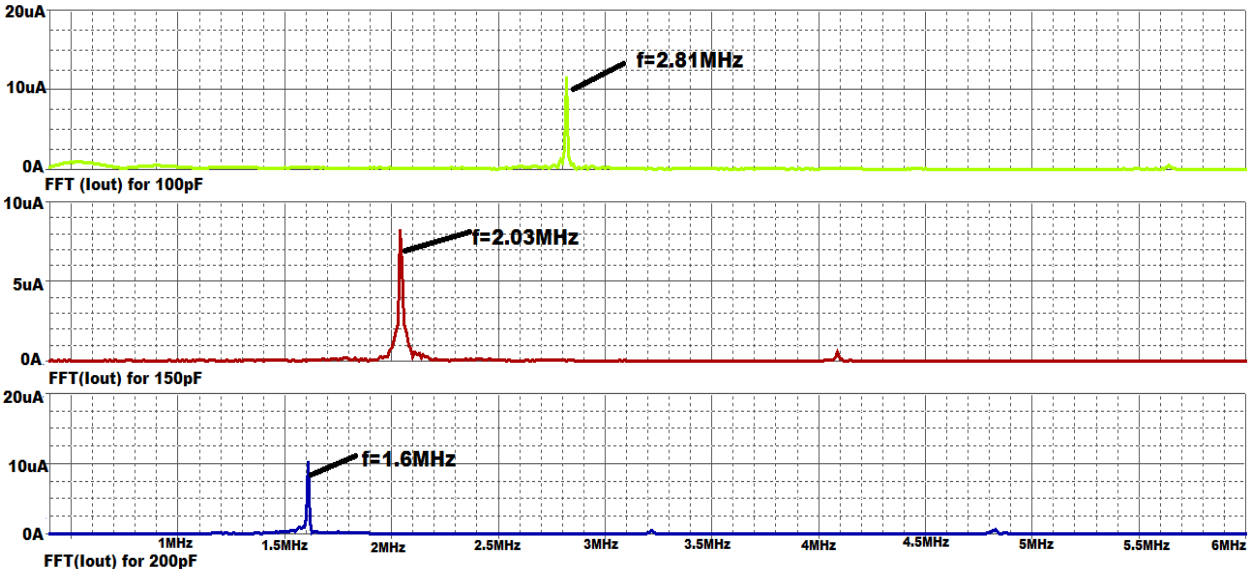

Figure 16. The frequency spectrum of the proposed triangle generator for different capacitor values**.**

4.3 Non-Idealities Effects and Parasitic Effects

For a more precise evaluation, the outcome of non-idealities and parasitic present in the CFTA-based design **Fig. 3** are to be considered. The occurrence of non-idealities is due to the presence of a mismatch in the MOS transistors. By allowing for the non-idealities characteristics of the CFTA, the kinship of the voltages and currents can be rephrased as:

$$\begin{bmatrix} V_f \\ I_z \\ I_{x+} \\ I_{x-} \end{bmatrix} = \begin{bmatrix} 0 & 0 & 0 & 0 \\ \alpha i & 0 & 0 & 0 \\ 0 & +\beta_v g_m & 0 & 0 \\ 0 & -\beta_v g_m & 0 & 0 \end{bmatrix} \cdot \begin{bmatrix} I_f \\ V_Z \\ V_{x+} \\ V_{x-} \end{bmatrix}$$

where $\propto_i = 1 - \varepsilon_i$ and ε_i ($|\varepsilon_i| \ll 1$) indicate the current gain and $\beta_v = 1 - \varepsilon_v$ and ε_v ($|\varepsilon_v| \ll 1$) indicate the voltage gain. The ideal gain tracking errors are $\propto_i$ and β_v for a system, emphasizing that they should be unity. The parasitic impedances at ports Z and X, represented as Z and X are R_Z //C_Z and R_X //C_X respectively. Assuming that (R_F) at port F to be zero for simplicity. The impedances R_Z and R_X are treated as infinite, and the capacitance (C_X) is nearly zero. Additionally, the capacitance (C_Z) is noted to influence the total capacitance when added in parallel with another capacitor, and a non-ideal equivalent circuit is shown in **Fig. 17**.

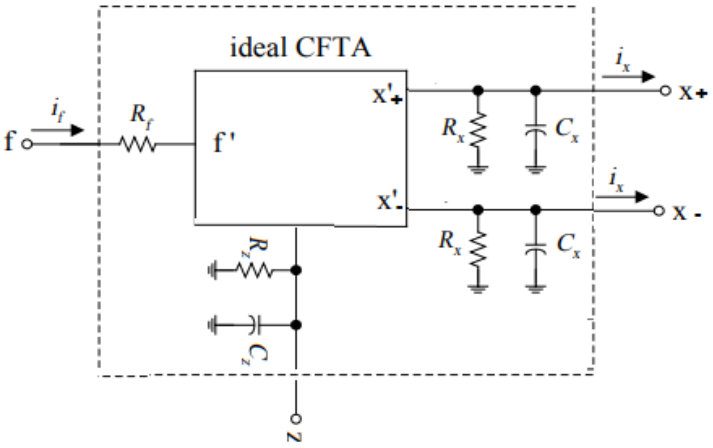

Figure 17. Equivalent circuit of the non-ideal CFTA.

The performance of the circuit is significantly affected by various factors such as parasitic capacitances and resistances, along with the non-ideal characteristics of MOS transistors. These elements contribute to the overall tracking error. Understanding these influences is essential for optimizing circuit design and improving overall functionality re-analysis of the square and triangle waveform generator circuit yields the modified transfer function and frequency of oscillation.

$$Transfer\ function = \frac{\beta_1\beta_2\alpha_1\alpha_2 g_{m1}g_{m2}R}{\beta_1\beta_2\alpha_1\alpha_2 g_{m1}g_{m2}R + S((C+C_Z) - \beta_1\alpha_1 g_{m1}R(C+C_Z)} \quad (10)$$

$$f = \frac{\beta_1\beta_2\alpha_1\alpha_2 g_{m1}g_{m2}R}{2\pi(C+C_Z)\,(\beta_1\alpha_1 g_{m1}R - 1)} \quad (11)$$

From Eqs. 10 and 11, it is appreciated that the transfer function may deviate from the ideal one due to various parasitic effects and non-idealities.

5. CONCLUSIONS

The proposed circuit presents a current mode Schmitt trigger circuit and its application to square and triangular wave generators that utilize a Current Follower Transconductance Amplifier (CFTA), highlighting its benefits such as simplicity, low power consumption, wide bandwidth, and adjustable thresholds. The functionality of the proposed circuit is validated through PSPICE simulations, demonstrating its effectiveness in practical applications. The proposed circuit ensures low power consumption while maintaining performance through some mechanisms. By using only active elements and grounded resistors, the circuit minimizes power losses typically associated with passive components. The design is specifically optimized for low-voltage operation, which inherently reduces power

consumption. The Current Follower-Transconductance Amplifier (CFTA) allows for efficient current handling, which contributes to lower overall power usage without sacrificing performance. The ability to operate over a wide bandwidth means that the circuit can respond quickly to changes, reducing the need for excessive power to maintain performance. These factors collectively contribute to the circuit's ability to operate efficiently while delivering high performance.

NOMENCLATURE

Symbol	Description	Symbol	Description
g_m	Transconductance gain	R_Z	Resistance at Z terminal (ohm)
V_T	Thermal voltage (Volt)	I_B	Bias Current (Amper)

Acknowledgements

This work was supported by (Department of Electrical Engineering at Salahaddin University), by PSPICE program.

Declaration of Competing Interest

The author announce that has no no known competing financial interests or personal relationships that could have appeared to influence the work described in this paper.

REFERENCES

Akter, M., Reaz, M., and Choong, F., 2008. Hardware implementations of an image compressor for mobile communications. *Journal of Communications Technology and Electronics*, 53(8), pp. 899-910. http://dx.doi.org/10.1134/S106422690808007X.

Amiri, P., Nabavi, A., and Mortazavi, S. Y., 2010. Low distortion CMOS class-D amplifier with double-band hysteresis. *IEICE Electronics Express,* 7(4), pp. 273-280. https://doi.org/10.1587/elex.7.273

Bang, J., Song, J.H., and Lee, W. C., 2014. Analyzing of CDTA using a new small signal equivalent circuit and application of LP filters. *Journal of the Korea Academia-Industrial Cooperation Society*, 15(12), pp. 7287-7291. https://doi.org/10.5762/KAIS.2014.15.12.7287.

Başak, M.E., Özer, E., 2022. Electronically tunable grounded inductance simulators and capacitor multipliers realization by using a single Current Follower Transconductance Amplifier (CFTA). *Analog Integr Circ Sig Process*, 112, pp. 401–415. https://doi.org/10.1007/s10470-022-02049-4.

Biolek, D., 2003. CDTA-building block for current-mode analog signal processing. *In Proceedings of the ECCTD* Vol. 3, pp. 397-400.

Chavez, S. R., 1995. Mixed-mode Schmitt trigger equivalent circuit. *Electronics Letters*, 31(3), PP. 152-154. https://doi.org/10.1049/el:19950107.

Choi, H., Song, K., Jeong, Y., Kenney, J. S., and Kim, C.D., 2009. Propagation delays matched CMOS 0.18 μm frequency doubler for L-band application. *Microwave and Optical Technology Letters*, 51(7), pp. 1729-1732. https://doi.org/10.1002/mop.24420.

Daibor, B., raj, S., Viera, B., and Zdenek, K., 2008. Active elements for analog signal processing: classification, review, and new proposals. *Radioengineering*, 17(4), pp. 15-32.

Das, R., Kumar, H., Giri, A. K., and Prasad, A., 2017. Current mode Schmitt trigger circuit design using only single CCCDTA. *International Journal of Advanced Engineering and Management*, 2(9), pp. 219-222. https://doi.org/10.24999/IJOAEM/02090049.

De Marcellis, A., Ferri, G., and Mantenuto, P., 2017. A CCII-based non-inverting Schmitt trigger and its application as astable multivibrator for capacitive sensor interfacing. *International Journal of Circuit Theory and Applications*, 45(8), pp. 1060-1076. https://doi.org/10.1002/cta.2268.

Demirel, H., Ahmed, A., 2023. New finFet transistor implementation of floating and grounded inductance simulator based on active elements. *Gazi Mühendislik Bilimleri Dergisi*, 9(3), pp. 647-653. http://dx.doi.org/10.30855/gmbd.0705095.

Fathima, R., Perumal, S.P., Muniyappan, V., Faseehuddin, M., and Tangsrirat, W., 2022. Electronically tunable multifunction current mode filter employing grounded capacitors. *Informacije MIDEM*, 52(4), pp. 205-214. https://doi.org/10.33180/InfMIDEM2022.401.

Janveja, M., Khan, A., and Niranjan, V., 2016. Performance evaluation of subthreshold Schmitt trigger using body bias techniques. In 2016 *International Conference on Computational Techniques In Information And Communication Technologies (ICCTICT) (pp. 486-489). IEEE.* https://doi.org/10.1109/ICCTICT.2016.7514629.

Kannaujiya, A., Singh, A.P., and Shah, A.P., 2024. Noninverting Schmitt trigger circuit with electronically tunable hysteresis. *Microelectronics Journal*, 144, https://doi.org/10.1016/j.mejo.2023.106073.

Keskin, A. Ü., Biolek, D., Hancioglu, E., and Biolková, V., 2006. Current-mode KHN filter employing current differencing transconductance amplifiers. *AEU-International Journal of Electronics and Communications*, 60(6), pp. 443-446. https://doi.org/10.1016/j.aeue.2005.09.003.

Kumar, A., Chaturvedi, B., 2017. Fully electronically controllable Schmitt trigger circuit with dual hysteresis, *Electronics Letters*, 53(7), pp. 459–461. https://doi.org/10.1049/el.2016.4770.

Kumar, A., Chaturvedi, B., 2017. Novel electronically controlled current-mode Schmitt trigger based on a single active element. *AEU-International Journal of Electronics and Communications*,*82*, pp.160-166. https://doi.org/10.1016/j.aeue.2017.08.007

Kumari, S., Gupta, M., 2017. Design and analysis of high transconductance current follower transconductance amplifier (CFTA) and its applications. *Analog Integrated Circuits and Signal Processing*, 93, pp. 489-506. https://doi.org/10.1007/s10470-017-1036-x.

Lin, Y., Gong, J., Yu, F., and Huang, Y., 2023. Current mode multi-scroll chaotic oscillator based on CDTA. *Frontiers in Physics*, 11. https://doi.org/10.3389/fphy.2023.1202398.

Madira, S., Reddy, V.V. and Srinivasulu, A., 2016. Current mode Schmitt trigger based on ZC-current differencing transconductance amplifier. In 2016 *International Conference on Inventive Computation Technologies (ICICT) (Vol. 1, pp. 1-5). IEEE*. https://doi.org/10.1109/INVENTIVE.2016.7823226.

Maheswari, K., Srinivasulu, A., and Ravariu, C., 2019. Z-copy current differencing buffered amplifier-based Schmitt trigger circuit without passive components. *Solid State Electronics Letters* 1, pp. 140–146. https://doi.org/10.1016/j.ssel.2019.11.003.

Mohammed, A.A., Mahmood, Z.K., and Demirel, H., 2024. New Z copy-current differencing transconductance amplifier active filter using FinFET transistor-based current Mode Universal Filter. *Global Journal of Engineering and Technology Advances*, 18(2), pp. 001-005. https://doi.org/10.30574/gjeta.2024.18.2.0019.

Nagalakshmi, K., Avireni, S., Cristian, R., Vijay, V., and Krishna, V., 2018. A novel simple Schmitt trigger circuit using CDTA and its application as a square-triangular waveform generator. *Journal of Modern Technology and Engineering*, 3(3), pp. 205-216.

Nisha, W., Syed, N., 2015. Realization of a new current mode second-order biquad using two current follower transconductance amplifiers (CFTAs). *Circuits and Systems*, 6, pp. 113-120. http://dx.doi.org/10.4236/cs.2015.65012.

Özer, E., 2021. Electronically tunable CFTA-based positive and negative grounded capacitance multipliers. *AEU-International Journal of Electronics and Communications*, 134. https://doi.org/10.1016/j.aeue.2021.153685.

Pal, R., Pandey, R., Pandey, N., and Tiwari, R.C., 2015. Single CDBA-based voltage mode bistable multivibrator and its applications. *Circuits and Systems*, 6(11), pp. 237-251. http://dx.doi.org/10.4236/cs.2015.611024.

Prasad, S.S., Kumar, P., and Ranjan, R.K., 2021. Resistorless memristor emulator using CFTA and its experimental verification. *IEEE Access*, 9, pp. 64065-64075. https://doi.org/10.1109/ACCESS.2021.3075341.

Ranjan, A., Pamu, H., and Tarunkumar, H., 2018. A novel Schmitt trigger and its application using a single four-terminal floating nullor (FTFN). *Analog Integrated Circuits Signal Process*. 96(3), pp. 455–467. https://doi.org/10.1007/s10470-018-1229-y.

Radfar, S., Nejati, A., Bastan, Y., Amiri, P., Maghami, M. H., Nasrollahpour, M., and Hamedi-Hagh, S., 2020. A sub-threshold differential CMOS Schmitt trigger with adjustable hysteresis based on body bias technique. *Electronics, 9(5), 806.* https://doi.org/10.3390/electronics9050806

Sotner, R., Petrzela, J., and Slezak, J., 2009. Current mode tunable KHN filter based on controlled MO-CFTAs. *In 2009 3rd International Conference on Signals, Circuits and Systems (SCS) (pp. 1-4). IEEE*. https://doi.org/10.1109/ICSCS.2009.5414170.

Silapan, P., Chanapromma, C., 2011. Multiple output CFTAs (MO-CFTAs)-based wide-range linearly/electronically controllable current-mode square-rooting circuit. *In 2011 International Symposium on Intelligent Signal Processing and Communications Systems (ISPACS) (pp. 1-4). IEEE*. https://doi.org/10.1109/ISPACS.2011.6146152.

Singh, S.V., Tomar, R.S., and Chauhan, D.S., 2013. Single MO-CFTA-based current-mode SITO biquad filter with electronic tuning. *International Journal of Computer Science and Information Security*, 11(4), P. 77.

Singh, S.V., Tomar, R.S., and Chauhan, D.S., 2016. Single CFTA-based current-mode universal biquad filter. *The Journal of Engineering Research [TJER]*, 13(2), pp. 172-186. https://doi.org/10.24200/tjer.vol13iss2pp172-186.

Siripruchyanun, M., Satthaphol, P., and Payakkakul, K., 2015. A simple fully controllable Schmitt trigger with electronic method using VDTA. *Applied Mechanics and Materials*, 781, pp. 180-183. https://doi.org/10.4028/www.scientific.net/AMM.781.180.

Srinivasulu, A., Zahiruddin, S., and Sarada, M., 2020. A novel dual output Schmitt trigger using second generation current controlled conveyor. *Electronics Journal*, 24(1), pp. 49-54. https://doi.org/10.7251/ELS2024047S.

Tangsrirat, W., Dumawipata, T., and Surakampontorn, W., 2007. Multiple-input single-output current-mode multifunction filter using current differencing transconductance amplifiers. *AEU-*

International Journal of Electronics and Communications, 61(4), pp. 209-214. https://doi.org/10.1016/j.aeue.2006.04.004.

Tasneem, S., Ranjan, R.K., and Paul, S.K., 2022. Performance enhancement of current follower transconductance amplifier (CFTA) and its application as filter. *Journal of Circuits, Systems and Computers*, 31(02), P. 2250024. https://doi.org/10.1142/S0218126622500244.

Thakur, R., Singh, S., 2021. Voltage tunable current mode KHN filter based on current differencing transconductance amplifier (CDTA). *International Journal of Modern Physics B*, 35(17), P. 2150181. https://doi.org/10.1142/S0217979221501812.

Wassan, M., Haroon, R., Mamun, M., and Mohammad, A.S., 2012. Advancement of CMOS schmitt trigger circuits. *Modern Applied Science*, 6(12), pp. 51-58. http://dx.doi.org/10.5539/mas.v6n12p51.

Yuan, F., 2009. Current regenerative Schmitt triggers with tunable hysteresis. *In 2009 52nd IEEE International Midwest Symposium on Circuits and Systems (pp. 110-113). IEEE*. https://doi.org/10.1109/MWSCAS.2009.5236141.

Yuan, F., 2010a. A high-speed differential CMOS Schmitt trigger with regenerative current feedback and adjustable hysteresis. *Analog Integrated Circuits and Signal Processing,* 63, pp.121-127. https://doi.org/10.1007/s10470-009-9374-y.

Yuan, F., 2010b. Differential CMOS Schmitt trigger with tunable hysteresis. *Analog Integrated Circuits and Signal Processing,* 62, pp. 245-248. https://doi.org/10.1007/s10470-009-9366-y

تحقيق دارة تشغيل شميت المقلوبة وغير المقلوبة في الوضع التيار باستخدام مضخم توصيل الموصلية التابع للتيار (CFTA)

اميره رمزى حمد

قسم الهندسة الكهربائية، كلية الهندسة، جامعة صلاح الدين، اربيل، العراق

الخلاصة

اقترحت هذه المقالة وضع التيار المقلوب وغير المقلوب لدائرة تشغيل شميت في وقت واحد والتي تستخدم مضخم توصيل التيار التابع (CFTA) واستخدامه لمولدات الموجات المربعة والمثلثة لأن تباطؤ مشغل شميت يتأثر بشكل مباشر بتغيرات العملية وعدم تطابق الترانزستور. تعتبر هذه المشكلة أكثر إشكالية في التطبيقات التي لا يمكن التنبؤ بمستوى الضوضاء والاضطرابات فيها. للتغلب على هذا النقص، يمكن استخدام مشغلات شميت مع التباطؤ القابل للضبط كحل مفيد. تتكون الدائرة المقترحة من وحدة بناء تناظرية CFTA واحدة بشكل جانبي مع مقاومة مؤرضة واحدة. المقاوم المؤرض يجعل الدائرة المقترحة ممكنة من منظور البناء. تحتوي الدائرة المقترحة على مدخلات منخفضة بالإضافة إلى ممانعات خرج عالية، وهو المفضل في دائرة وضع التيار (CM). ويتميز بعتبات قابلة للتعديل، والحد الأدنى من استهلاك الطاقة، وتوفير استجابات مقلوبة وغير مقلوبة بدون عناصر عائمة إضافية، ومستويات عتبة قابلة للتعديل إلكترونيًا، وعرض نطاق واسع، وكلها تم التحقق من صحتها من خلال محاكاة PSPICE. يركز التصميم على تقليل فقد الطاقة من خلال دمج العناصر النشطة والمقاومات المؤرضة، وتحسينها لتشغيل الجهد المنخفض مع إدارة التيار بشكل فعال لضمان الأداء العالي دون الاستخدام المفرط للطاقة. تقديم طريقة فعالة ومنخفضة الطاقة لتوليد موجات مربعة ومثلثة. تم توضيح نتائج محاكاة PSPICE، وتتوافق النتائج المعطاة بشكل جيد مع التوقعات النظرية. يبلغ إجمالي تبديد الطاقة حوالي 1.26 ميجاوات عند جهد إمداد ± 1.5 فولت.

الكلمات المفتاحية: الزناد شميت، مضخم توصيل التيار التابع للتيار، نمط التيار